Protein-Protein Interactions Contributing to the Specificity of Intracellular Vesicular Trafficking

Nicole Calakos, Mark K. Bennett, Karen E. Peterson, Richard H. Scheller

Intracellular vesicles destined to fuse with the plasma membrane and secrete their contents must have a mechanism for specifically interacting with the appropriate target membrane. Such a mechanism is now suggested by the demonstration of specific interaction between vesicular proteins and plasma membrane proteins. The vesicle-associated membrane proteins (VAMPs) 1 and 2 specifically bind the acceptor membrane proteins syntaxin 1A and 4 but not syntaxin 2 or 3. The binding site is within amino acids 194 to 267 of syntaxin 1A, and the approximate equilibrium dissociation constant is 4.7×10^{-6} molar. These data suggest a physical basis for the specificity of intracellular vesicular transport.

The secretory pathway of eukaryotic cells consists of distinct compartments with unique membrane and cargo compositions. This organization is believed to arise from the sorting of restricted sets of molecules into particular transport vesicles, followed by the targeting of these vesicles to the appropriate acceptor compartment. After vesicle targeting, fusion of the lipid bilayers results in the transfer of the vesicle membrane and cargo to the acceptor compartment. The specificity of this targeting and fusion reaction likely involves an interaction between molecules on transport vesicles and target (acceptor) membranes.

The most completely characterized transport vesicle is the synaptic vesicle of neurons (*1–3*). VAMP 1 and 2 (*4, 5*), also called synaptobrevin (*6, 7*), are proteins of the synaptic vesicle membrane that have been proposed to participate in vesicle docking and fusion. The neuron-specific plasma membrane proteins syntaxin 1A and 1B have been hypothesized to be plasma membrane receptors for synaptic vesicles (*8*). Their role in the docking and fusion of synaptic vesicles is further supported by the fact that they are each targets of clostridial neurotoxins that block neurotransmitter release (*9*). The possibility that VAMPs and syntaxins are involved more broadly in membrane trafficking is supported by the existence of multiple members of the VAMP and syntaxin gene families (*10, 11*), the broad tissue expression of these genes (*10–12*), and their homology to yeast proteins known to participate in secretion (*13–17*). Furthermore, VAMP and syntaxin are part of a membrane protein complex that interacts with the soluble proteins *N*-ethylmaleimide–sensitive factor (NSF) and soluble NSF attachment proteins (SNAPs), which regulate the fusion of membranes (*18, 19*).

We investigated the possibility that an interaction between VAMP and syntaxin proteins contributes to the specificity of vesicle targeting. Epitope-tagged forms of VAMP 2 (FLAG epitope) and syntaxin 1A, 2, and 4 [hemagglutinin (HA) epitope] were expressed in COS cells. Each of the three syntaxin constructs was individually cotransfected with the VAMP 2 construct. To examine a potential interaction between the transfected gene products, we subjected detergent-solubilized lysates of the transfected cells to immunoprecipitation with antibody to the FLAG epitope (VAMP 2) or the HA epitope (syntaxins). The amount of precipitated VAMP 2 and syntaxin was determined by Western blot analysis (Fig. 1). Although the immunoprecipitation of syntaxin 1A and syntaxin 4 resulted in the coprecipitation of VAMP 2, immunoprecipitation of syntaxin 2 did not. Consistent with this analysis, immunoprecipitation of VAMP 2 resulted in the coprecipitation of syntaxin 1A and 4 but not syntaxin 2. These data suggest that VAMP 2 can form specific complexes with certain syntaxins.

To determine whether this coprecipitation reflects a direct interaction between VAMP and syntaxin, we performed binding experiments with bacterially expressed recombinant proteins. Glutathione-S-transferase (GST) fusion proteins containing the cytoplasmic domains, an amino-terminal portion of the cytoplasmic domains, or a carboxyl-terminal portion of the cytoplasmic domains of syntaxin 1A, 2, 3, and 4 were synthesized and bound to glutathione agarose (Fig. 2A). The recombinant portions of GST fusion proteins containing the cytoplasmic domains of VAMP 1 and 2 were purified and incubated with the syntaxin-containing beads. The binding of VAMP to the syntaxin-agarose beads was detected by Western blot analysis

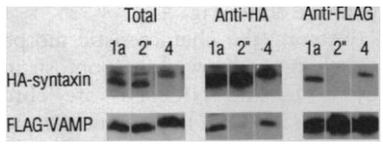

Fig. 1. Syntaxin 1A and 4 form complexes with VAMP 2. COS cells were transiently transfected with DEAE-dextran as described (*11*). Each plasmid encoding full-length syntaxin isoforms tagged with the HA epitope (1A, 2, or 4) was cotransfected with a plasmid encoding full-length VAMP 2 tagged with the FLAG epitope (*35*). At a time of 36 hours after transfection, the cells were lysed in 10 mM Hepes-KOH (pH 7.5), 140 mM potassium acetate, 1 mM $MgCl_2$, 0.1 mM EGTA with 2% Triton X-100. The lysates were immunoprecipitated with monoclonal antibodies against HA (12CA5) (*36*) or FLAG (M2, International Biotechnologies). After three washes, the immunoprecipitate was eluted with SDS sample buffer and analyzed by SDS–polyacrylamide gel electrophoresis (PAGE) and Western blotting; the first panel is 10% of the total material incubated in each immunoprecipitation. Syntaxin and VAMP 2 were visualized with antibodies to HA and VAMP (*12*), respectively.

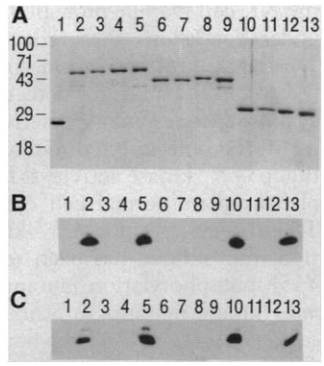

Fig. 2. Interaction of recombinant VAMP with syntaxin 1A and 4. (**A**) Coomassie blue–stained polyacrylamide gel of GST-syntaxin fusion proteins (*37*) after affinity chromatography with glutathione agarose. For (A) to (C): lane 1, GST alone; lanes 2 to 5, GST with the cytoplasmic domain of syntaxin 1A (amino acids 4 to 267), 2 (4 to 264), 3 (4 to 264), or 4 (5 to 274), respectively; lanes 6 to 9, GST with an amino-terminal portion of the cytoplasmic domain of syntaxin 1A (4 to 193), 2 (4 to 191), 3 (4 to 187), or 4 (5 to 196), respectively; lanes 10 to 13, GST with a carboxyl-terminal portion of the cytoplasmic domain of syntaxin 1A (194 to 267), 2 (192 to 264), 3 (188 to 264), or 4 (197 to 274), respectively. (**B**) Immunoblot analysis of VAMP 2 binding. Purified cytoplasmic fragment of VAMP 2 (amino acids 1 to 94) (*38*) was added in equal amounts to GST-syntaxin fusion proteins bound to glutathione agarose. After a 2-hour incubation at 4°C in 10 mM Hepes (pH 7.4), 150 mM NaCl, 0.05% Tween-20 (HBS-T20) with excess bovine serum albumin and gelatin (1 mg ml^{-1} each), the beads were washed three times with HBS-T20, and the bound protein was eluted with SDS sample buffer and analyzed by SDS-PAGE and Western blot analysis with affinity-purified antibodies to VAMP (*12*). Approximately 0.6 mol of VAMP 2 bound per mole of cytoplasmic syntaxin 1A and 4 and 0.4 mol of VAMP 2 bound per mole of carboxyl domain of syntaxin 1A and 4. (**C**) Immunoblot analysis of VAMP 1 binding, as described above, but with the purified cytoplasmic fragment of VAMP 1 (amino acids 1 to 96).

Howard Hughes Medical Institute, Department of Molecular and Cellular Physiology, Stanford University Medical Center, Stanford, CA 94305, USA.

(Fig. 2B). Consistent with the COS cell results, VAMP 1 and 2 bound the cytoplasmic domain of syntaxin 1A and 4. VAMP 1 and 2 did not interact with syntaxin 2, syntaxin 3, or a GST control. The amino-terminal domains of all four syntaxins failed to bind either VAMP 1 or 2, whereas the carboxyl-terminal domains of syntaxin 1A and 4, but not of syntaxin 2 or 3, bound both VAMP 1 and 2. These data suggest that the formation of complexes between the vesicular VAMPs and the plasma membrane syntaxins arises from a direct interaction between these molecules. The observation that VAMPs interact with some syntaxins but not with others suggests that at least one component of the specificity of vesicular trafficking may be encoded in these interactions.

To understand further the binding of VAMP and syntaxin, we studied their interactions by using surface plasmon resonance (SPR) detection (*20–22*). This technique measures the real-time association and dissociation of molecules on a sensor surface and allows estimates of kinetic binding constants. The purified recombinant proteins used in this assay are shown in Fig. 3. The cytoplasmic domain of VAMP 2 was immobilized to the flow cell of the sensor surface. The cytoplasmic, amino-, and carboxyl-terminal domains of syntaxin 1A were examined for their ability to bind the immobilized VAMP 2. The carboxyl-terminal domain of syntaxin 1A interacted with the VAMP 2. No binding was observed with either the cytoplasmic or amino-terminal domains of syntaxin 1A (Fig. 4A), a GST control preparation, bovine serum albumin, or cytochrome c. Concentration-dependent binding of the carboxyl-terminal syntaxin 1A fragment was observed and used to calculate kinetic rate constants (Fig. 4, B and C) (*23*, *24*). The association rate constant, k_a, was 470 ± 50 M^{-1} s^{-1} (SEM) (n = 13). The dissociation rate constant, k_d, was $2.2 \times 10^{-3} \pm 0.3 \times 10^{-3}$ s^{-1} (SEM) (n = 6). From these data, the calculated dissociation equilibrium constant ($K_D = k_d/k_a$) is 4.7 μM.

To investigate the absence of binding between the cytoplasmic domain of syntaxin 1A and VAMP 2, we mixed the amino- and carboxyl-terminal fragments of syntaxin 1A before injection into the VAMP 2 flow cell. The inclusion of the amino-terminal fragment caused a dose-dependent inhibition of the binding of the carboxyl-terminal fragment to the immobilized VAMP 2 (Fig. 5A). The amino-

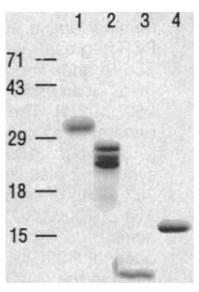

Fig. 3. Purified recombinant VAMP 2 and syntaxin 1A protein fragments. Coomassie blue–stained polyacrylamide gel of the following samples: lane 1, syntaxin 1A cytoplasmic domain (amino acids 4 to 267); lane 2, syntaxin 1A amino-terminal domain (4 to 193); lane 3, syntaxin 1A carboxyl-terminal domain (194 to 267); and lane 4, VAMP 2 cytoplasmic domain (1 to 94) (*37*, *38*). Although the amino-terminal domain of syntaxin 1A is a single fusion protein (see Fig. 2A), three bands are reproducibly observed after thrombin cleavage that is required to isolate the recombinant fragment (lane 2).

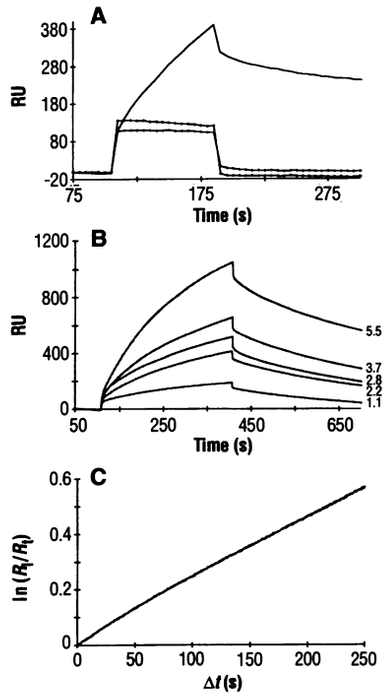

Fig. 4. Real-time SPR detection of the VAMP 2 and syntaxin 1A interaction. (**A**) Resonance units (RU) are plotted as a function of time (sensorgrams) for representative experiments: The carboxyl domain (9 μM) (top trace), the cytoplasmic domain (3 μM) (middle trace), and the amino-terminal domain (8 μM) (bottom trace) of syntaxin 1A were injected into a flow cell containing the immobilized cytoplasmic domain of VAMP 2. No interaction was seen with the cytoplasmic or amino-terminal domains at any concentration tested, up to 30 μM. The sharp vertical rise in RU at the beginning and end of the sample injection corresponds to the refractive index change between the sample and the flow buffer (*39*). (**B**) Sensorgrams of the carboxyl-terminal domain of syntaxin 1A binding to VAMP 2 (concentrations of syntaxin 1A are given to the right of each trace in micromolarity). A total of 2400 RU of VAMP 2 cytoplasmic domain was immobilized to the flow cell (*39*). The flow rate was 5 μl min^{-1} during the association phase and 30 μl min^{-1} during the dissociation phase. The higher flow rate during dissociation was chosen to minimize the possibility of analyte rebinding to the immobilized ligand. (**C**) Plot of ln (R_i/R_t) as a function of Δt, a linearizing transformation of the dissociation phase of the carboxyl-terminal domain of syntaxin 1A (5.5 μM) binding to VAMP 2 in the experiment in Fig. 4B (R_i = initial response, R_t = resonance units at time Δt, the time after the start of dissociation phase). The dissociation rate was obtained by averaging the slopes obtained from such an analysis of six experiments.

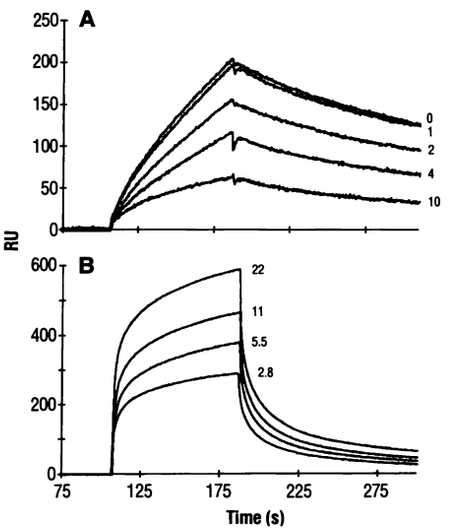

Fig. 5. Amino- and carboxyl-terminal domains of syntaxin 1A interact and prevent VAMP 2 binding. (**A**) Sensorgrams of syntaxin 1A carboxyl-terminal domain (5.5 μM) binding to immobilized VAMP 2 cytoplasmic domain in the presence of increasing amounts of syntaxin 1A amino-terminal domain [in (A) and (B), concentrations are given to the right of each trace in micromolarity]. The data are derived by subtraction of the values obtained from the binding of syntaxin 1A to VAMP 2 from that of syntaxin 1A binding to a negative control surface, which removes the RU change due to the refractive index of the injected sample. The spikes at the start of dissociation are an artifact created by the subtraction, because the injection pulses were not exactly coincident between experiments. The inhibitory constant (IC_{50}) of the amino-terminal syntaxin 1A in this experiment is approximately 3 μM. A total of 2400 RU of VAMP 2 cytoplasmic domain was immobilized on the flow cell. The control surface was an identical immobilization of a lysate expressing GST only, which was prepared exactly as was the VAMP 2 lysate. The samples were preincubated on ice for 2 hours. The injection was 15 μl min^{-1} at room temperature. A control preparation (lysate expressing only GST) when added to the syntaxin 1A carboxyl-terminal domain under identical conditions did not inhibit the binding to VAMP 2, nor did the addition of the syntaxin 1A amino-terminal domain block the interaction of rabbit immunoglobulin G with immobilized protein A. (**B**) Sensorgrams of syntaxin 1A carboxyl-terminal domain binding to immobilized syntaxin 1A amino-terminal domain. A total of 11,000 RU of syntaxin 1A amino-terminal domain was immobilized. The injection was 15 μl min^{-1} at room temperature. Kinetic rate constants (*23*) were $k_a = 2.2 \times 10^3 \pm 0.7 \times 10^3$ M^{-1} s^{-1} (SEM), n = 8; and $k_d = 9 \times 10^{-3} \pm 0.8 \times 10^{-3}$ s^{-1} (SEM), n = 8. The K_D was 4.1 μM.

terminal fragment of syntaxin 1A may bind the carboxyl-terminal fragment and thereby prevent the interaction with VAMP 2. To test this hypothesis, the amino-terminal fragment of syntaxin 1A was immobilized to the flow cell and the carboxyl-terminal fragment of syntaxin 1A was examined for binding activity. A dose-dependent binding of amino-terminal to carboxyl-terminal fragments of syntaxin 1A was observed (Fig. 5B). These data suggest that under the conditions of the SPR analysis, the cytoplasmic domain of syntaxin 1A is folded so that the amino-terminal region binds a domain in the carboxyl-terminal region of the protein and that this folding inhibits binding to VAMP 2. There are several experimental conditions of the SPR analysis that differ from those of the COS cell transfection studies and GST-syntaxin chromatography experiments that could account for a difference in the ability to detect an interaction between VAMP and the full cytoplasmic portion of syntaxin. These conditions include the duration of exposure of VAMP to syntaxin (minutes versus hours), the temperature of the assay (25° versus 4°C), the protein that was immobilized, and the method of immobilization. Each of these factors could significantly alter the prevalence of a particular syntaxin conformational state. Perhaps the syntaxin protein exists in vivo in a series of conformations that regulate VAMP binding and therefore vesicle targeting.

In this report, we demonstrate that VAMP and the plasma membrane–localized syntaxin directly bind each other in vitro. VAMP 2 interacts both in COS cells and in vitro with syntaxin 1A and 4 but not syntaxin 2. We extended the analysis in vitro to show that VAMP 1 and 2 interact similarly with these syntaxins and do not bind to syntaxin 3. These data support the hypothesis that selective combinatorial associations of VAMPs and syntaxins may lend specificity to intracellular vesicular trafficking events. Only membrane compartments with correct combinations of these molecules should dock or fuse with each other.

Because a GST–VAMP 2 fusion protein containing only the central, highly conserved domain of VAMP is sufficient to bind syntaxin 1A (*25*), it is not surprising that the two VAMPs in this study behave similarly. More divergent VAMP proteins that could interact with the other syntaxins may have yet to be identified. Although syntaxin 1A is more closely related to syntaxin 2 and 3 than to syntaxin 4 (*11*), VAMP binds syntaxin 1A and 4. Thus, the specificity of these protein-protein interactions cannot be predicted from sequence similarities alone. Both VAMPs and syntaxins are predicted to have a high probability of forming coiled-coil protein structures (*26–28*). If these molecules interact by way of such structures, only one or a few amino acids may be critical for the binding.

The micromolar affinity for the interaction between VAMP 2 and syntaxin 1A is similar to that of other protein-protein interactions (*29–31*). Furthermore, synaptic vesicles have been suggested to be at micromolar concentrations in the brain (*32*). Thus, VAMP may be at a concentration of up to 10 μM, consistent with the measured affinity. In addition, the affinity reported here was determined with bacterially expressed soluble protein fragments. Native VAMP and syntaxin may have a higher affinity for each other. Finally, other components in the docking complexes (*18*) may contribute to the stability of the docked state.

A number of additional components, many of which are likely to be specific for particular steps in secretion (*33, 34*), are required to achieve the highly ordered process of vesicle targeting and fusion with acceptor membranes. Studies in yeast, mammalian cells, and the nervous system are in progress to define further the molecular basis of vesicular trafficking.

REFERENCES AND NOTES

1. R. B. Kelly, *Neuron* **1**, 431 (1988).
2. W. S. Trimble, M. Linial, R. H. Scheller, *Annu. Rev. Neurosci.* **14**, 93 (1991).
3. T. C. Sudhof and R. Jahn, *Neuron* **6**, 665 (1991).
4. W. S. Trimble, D. M. Cowan, R. H. Scheller, *Proc. Natl. Acad. Sci. U.S.A.* **85**, 4538 (1988).
5. L. A. Elferink, W. S. Trimble, R. H. Scheller, *J. Biol. Chem.* **264**, 11061 (1989).
6. M. Baumert, P. R. Maycox, F. Navone, P. DeCamilli, R. Jahn, *EMBO J.* **8**, 379 (1989).
7. T. C. Sudhof, M. Baumert, M. S. Perin, R. Jahn, *Neuron* **2**, 1475 (1989).
8. M. K. Bennett, N. Calakos, R. H. Scheller, *Science* **257**, 255 (1992).
9. W. Huttner, *Nature* **365**, 104 (1993).
10. H. T. McMahon *et al.*, *ibid.* **364**, 346 (1993).
11. M. K. Bennett *et al.*, *Cell* **74**, 863 (1993).
12. W. S. Trimble, T. S. Gray, L. A. Elferink, M. C. Wilson, R. H. Scheller, *J. Neurosci.* **10**, 1380 (1990).
13. M. K. Bennett and R. H. Scheller, *Proc. Natl. Acad. Sci. U.S.A.* **90**, 2559 (1993).
14. K. G. Hardwick and H. R. B. Pelham, *J. Cell Biol.* **119**, 513 (1992).
15. J. E. Gerst, L. Rodgers, M. Riggs, M. Wigler, *Proc. Natl. Acad. Sci. U.S.A.* **89**, 4338 (1992).
16. V. Protopopov, B. Govindan, P. Novick, J. E. Gerst, *Cell* **74**, 855 (1993).
17. M. K. Aalto, H. Ronne, S. Keranen, *EMBO J.* **12**, 4095 (1993).
18. T. Söllner, M. K. Bennett, S. W. Whiteheart, R. H. Scheller, J. E. Rothman, *Cell* **75**, 409 (1993).
19. T. Sollner *et al.*, *Nature* **362**, 318 (1993).
20. U. Jonsson *et al.*, *Biotechniques* **11**, 620 (1991).
21. L. G. Fagerstam, A. Frostell-Karlsson, R. Karlsson, B. Persson, I. Ronnberg, *J. Chromatogr.* **597**, 397 (1992).
22. S. C. Schuster, R. V. Swanson, L. A. Alex, R. B. Bourret, M. I. Simon, *Nature* **365**, 343 (1993).
23. The association rate data was fitted to the exponential equation

$$R_t = [Ck_aR_{max}/(Ck_a + k_d)] \times [1 - e^{-(Ck_a + k_d)/t}]$$

(*24*) with nonlinear least squares analysis software [Igor (WaveMetrics)]. This pseudo-first order interaction is appropriate: The analyte concentration is approximately constant, because it is continuously replenished by the sample injection flowing over the flow cell. Variables: R_t = resonance units (RU) at time t (in seconds), C = concentration of the injected analyte (M), R_{max} = maximum RU possible if the analyte bound 100% of the immobilized ligand. In no cases were the residual plots of the difference between the actual data and the predicted data greater than 10 RU, and most residuals were less than 4 RU in magnitude.
24. D. J. O'Shannessy, M. Brigham-Burke, K. K. Soneson, P. Hensley, I. Brooks, *Anal. Biochem.* **212**, 457 (1993).
25. N. Calakos and R. H. Scheller, unpublished observations with SPR detection: A recombinant VAMP 2 fusion protein (amino acids 25 to 94) interacts with the carboxyl-terminal domain of syntaxin 1A.
26. A. Inoue, K. Obata, K. Akagawa, *J. Biol. Chem.* **267**, 10613 (1992).
27. J. Spring, M. Kato, M. Bernfield, *Trends Biochem. Sci.* **18**, 124 (1993).
28. M. K. Bennett and A. E. Ting, unpublished observations with NEWCOILS [A. Lupas *et al.*, *Science* **252**, 1162 (1991)].
29. A. Fersht, *Enzyme Structure and Mechanism* (Freeman, New York, 1985), pp. 150–151.
30. J. L. Jorgensen, P. A. Reay, E. W. Ehrich, M. M. Davis, *Annu. Rev. Immunol.* **10**, 835 (1992).
31. A. P. Gilmore *et al.*, *J. Cell Biol.* **122**, 337 (1993).
32. R. Jahn and T. C. Sudhof, *J. Neurochem.* **61**, 12 (1993).
33. M. Zerial and H. Stenmark, *Curr. Opin. Cell Biol.* **5**, 613 (1993).
34. M. K. Aalto, S. Keranen, H. Ronne, *Cell* **68**, 181 (1992).
35. The complementary DNAs (cDNAs) for the full-length syntaxin isoforms 1A, 2, and 4 were subcloned into a derivative of the Bluescript II KS(−) plasmid, which contains an oligonucleotide encoding the HA epitope so that the epitope was at the amino-terminal end of the syntaxin isoforms (*11*). The cDNA for full-length VAMP 2 was subcloned into a derivative of Bluescript II KS(−) that contained an oligonucleotide encoding the FLAG epitope (International Biotechnologies) so that the epitope was at the amino-terminal end of the protein. The polylinker region between the region encoding the FLAG epitope and the start of VAMP 2 encoded eight additional amino acids, RPQIDTPA. The chimeric genes were directionally subcloned into the pCMV expression vector [S. Andersson *et al.*, *J. Biol. Chem.* **264**, 8222 (1989)]. Single-letter abbreviations for the amino acid residues are: A, Ala; C, Cys; D, Asp; E, Glu; F, Phe; G, Gly; H, His; I, Ile; K, Lys; L, Leu; M, Met; N, Asn; P, Pro; Q, Gln; R, Arg; S, Ser; T, Thr; V, Val; W, Trp; and Y, Tyr.
36. J. Field *et al.*, *Mol. Cell. Biol.* **8**, 2159 (1988).
37. The constructs encoding the cytoplasmic, amino-terminal, and carboxyl-terminal domains of syntaxin 2, 3, and 4 and the cytoplasmic domains of VAMP 1 and 2 were generated by polymerase chain reaction (PCR) with oligonucleotides encoding the amino- and carboxyl-terminal amino acids described in Fig. 2. The PCR fragments were directionally cloned into the Eco RI and Hind III sites of the pGEXKG vector [K. L. Guan and J. E. Dixon, *Anal. Biochem.* **192**, 262 (1991)]. The syntaxin 1A constructs were generated as described in M. K. Bennett *et al.* [*J. Neurosci.* **13**, 1701 (1993)]. The pGEXKG–syntaxin 2 plasmid encodes amino acids 265 to 267 (GVL) of syntaxin 2″ before the stop codon. The pGEXKG–VAMP 1 plasmid encodes amino acids 1 to 96 of VAMP 1. The additional sequence, GSPGISGGGGGI, is located amino terminal to the start of all fragments after thrombin cleavage of the GST fusion protein. The VAMP 2 recombinant protein contains the sequence, GSPGISGGGGGILDSMAELDTPA at the amino terminus after thrombin cleavage. All fusion proteins were expressed in the AB1899 strain of *Escherichia coli*.
38. Fusion proteins were expressed in the pGEXKG vector, and 1 liter of culture was prepared according to standard protocols [K. L. Guan and J. E.

Dixon, in (*37*)] with the following modifications: Fusion proteins were bound to glutathione agarose, and the recombinant portion was eluted for 30 min in 10 ml of 50 mM tris (pH 8.0), 150 mM NaCl, 2.5 mM $CaCl_2$, and 0.1% β-mercaptoethanol with thrombin (4 μg ml^{-1}). Phenylmethylsulfonyl fluoride (0.6 mM) was added to the protein elution, and the sample concentrated to 0.5 ml. The protein was further purified by gel filtration on a Superose 12 sizing column (Pharmacia, Piscataway, NJ) in HBS-T20 buffer. Control preparations were prepared identically from lysates expressing only the GST protein.

39. SPR detection experiments were performed with the BIAcore apparatus (Pharmacia Biosensor). All protein immobilizations were performed in 25 mM acetate buffer (pH 4.0), 15 mM NaCl, 0.05% Tween-20. The carboxylated dextran matrix of the flow cell was first activated with 1-ethyl-3-(3-dimethylaminopropyl)carbodiimide and *N*-hydroxysuccinimide, which allowed the subsequent cross-linking of injected protein through primary amine groups [B. Johnsson *et al.*, *Anal. Biochem.* **198**, 268 (1991)]. After the protein was cross-linked to the flow cell, the reactive groups were blocked by the injection of an excess of primary amines, 1 M ethanolamine (pH 8.5). Data for BIAcore SPR detection experiments were collected at 5 Hz. All binding was done in HBS-T20 buffer at room temperature.
40. We thank R. Granzow and J. Pevsner for critical support and discussions and S. Bajjalieh for editorial reading of the manuscript. Supported by the National Institute of Mental Health (R.H.S.). N.C. is a Medical Scientist Training Program trainee funded by the National Institute of General Medical Sciences.

17 November 1993; accepted 10 January 1994

Replacement of Diseased Mouse Liver by Hepatic Cell Transplantation

Jonathan A. Rhim, Eric P. Sandgren,* Jay L. Degen, Richard D. Palmiter, Ralph L. Brinster†

Adult liver has the unusual ability to fully regenerate after injury. Although regeneration is accomplished by the division of mature hepatocytes, the replicative potential of these cells is unknown. Here, the replicative capacity of adult liver cells and their medical usefulness as donor cells for transplantation were investigated by transfer of adult mouse liver cells into transgenic mice that display an endogenous defect in hepatic growth potential and function. The transplanted liver cell populations replaced up to 80 percent of the diseased recipient liver. These findings demonstrate the enormous growth potential of adult hepatocytes, indicating the feasibility of liver cell transplantation as a method to replace lost or diseased hepatic parenchyma.

Despite its highly specialized function, the liver is unique in its capacity to regenerate, even within the adult organism. The primary model of this process, two-thirds partial hepatectomy in the rat, has allowed investigation of molecular events that underlie the regenerative process (*1*). While much has been learned about liver regeneration, many questions regarding the proliferative capacity of adult liver cells remain. After partial hepatectomy, much of the lost liver mass is restored by the division of fully differentiated hepatocytes (*1, 2*). However, because only one to two rounds of hepatocellular division are required to restore the liver mass after partial hepatectomy, the extent of the regenerative capacity of hepatocytes is unknown. Certain pathological processes may reflect a finite capacity for hepatocyte replication. In gene therapy protocols, in which therapeutic genes are delivered to the liver via genetically modified hepatocytes, expression of the introduced gene declines over time (*3, 4*). This diminution of gene expression may be due to gradual loss of the modified cells because of a limited capacity to divide, either as a result of an inherent restriction in their replicative potential or as a result of changes acquired during their manipulation in culture, and is an especially serious problem given the very low colonization of host liver (less than 1%) that has been achieved in experimental models using hepatocellular transplantation (*3–5*). Finally, in conditions of severe liver injury, restoration of liver mass may be primarily accomplished not by hepatocytes but by the expansion of hepatocyte precursors (stem cells) that subsequently differentiate into hepatocytes. The existence of liver stem cells, their replicative potential, and their role in liver regeneration remain controversial (*6, 7*).

We recently described a model of liver regeneration in albumin-urokinase (Alb-uPA) transgenic mice [TgN(Alb1Plau)-144Bri, TgN(Alb1Plau)145Bri], in which hepatocyte-targeted expression of a hepatotoxic transgene creates a functional liver deficit (*8*) resulting in a chronic stimulus for liver growth. Because of the stimulus for liver growth present in these mice, a small number of hepatic cells in young mice that stochastically delete the deleterious transgene are selectively expanded. Each cell gives rise to a clone of hepatocytes that forms a nodule (*8*). By 8 to 12 weeks of age, transgenic mouse livers have been completely replaced by the nodular, clonal growth of these transgene-deficient cells (referred to as "red nodules"). The observation that the regenerating nodules in these livers were composed of normal appearing hepatocytes suggested that mature hepatocytes may indeed possess considerable replicative capacity. However, we could not rule out the possibility that the progenitor cells of these nodules, instead of being hepatocytes, were actually undifferentiated cells with a much greater replicative capacity than the hepatocytes to which they gave rise. Furthermore, even if nodule progenitor cells were hepatocytes, they were of fetal or early postnatal origin; cells at this stage display a much higher mitotic index than the adult hepatocytes, which are of greatest interest biologically and medically.

To determine the replicative capacity of adult liver cells, we transplanted cells isolated from adult mouse livers into Alb-uPA transgenic mice, then studied their growth. Marking of donor cells at the genetic level can be accomplished with retroviral transduction of hepatocytes (*9*), but for our studies we wished to avoid methods that might alter the replicative potential of the cells or mark only subpopulations of liver cells. We therefore transplanted cells freshly isolated from two groups of transgenic mice. The first, EL-*myc* [TgN(Ela1Myc)159Bri], carried the rat elastase enhancer-promoter fused to the mouse c-*myc* structural gene (*10*). This transgene is not expressed in liver; however, there are approximately nine copies per cell, facilitating detection of donor hepatocyte DNA within recipient livers. This lineage is congenic in C57BL/6 (B6). Second, we generated B6 donor transgenic mouse lines that carried the mouse metallothionein-I gene promoter plus flanking sequences fused to a modified β-galactosidase (β-gal) structural gene (MT-*lacZ*) (*11*). The protein product of this transgene is targeted to the cell nucleus as a result of the presence of the SV40 large T-antigen nuclear localization signal peptide. The MT promoter is active in liver of transgenic mice, and its expression can be induced up to 10-fold by administration of heavy metal

J. A. Rhim, Department of Animal Biology, School of Veterinary Medicine, University of Pennsylvania, Philadelphia, PA 19104, USA, and Department of Pathology and Laboratory Medicine, University of Pennsylvania School of Medicine, Philadelphia, PA 19104, USA.
E. P. Sandgren and R. L. Brinster, Department of Animal Biology, School of Veterinary Medicine, University of Pennsylvania, Philadelphia, PA 19104, USA.
J. L. Degen, Children's Hospital Research Foundation and Department of Pediatrics, University of Cincinnati College of Medicine, Cincinnati, OH 45229, USA.
R. D. Palmiter, Howard Hughes Medical Institute and Department of Biochemistry, University of Washington SL-15, Seattle, WA 98195, USA.

*Present address: Department of Pathobiological Sciences, School of Veterinary Medicine, University of Wisconsin–Madison, Madison, WI 53706, USA.
†To whom correspondence should be addressed.